Supplementary material for Wang et al.

Supplementary Table 1. Summary of properties of CARNs.

1. CARNs are a rare cell population			
	# Epithelial cells	**# Mice**	**# CARNs (Nkx3.1$^+$)**
Regressed prostate	38,329	4	266 *(0.7%)*

2. CARNs are luminal cells				
a. Luminal phenotype of CARNs				
Marker	**Cell type**	**# CARNs examined**	**# Mice**	**# CARNs expressing**
p63	basal	379	9	0 *(0%)*
Cytokeratin 18	luminal	837	4	828 *(99%)*
Synaptophysin	neuroendocrine	610	5	0 *(0%)*
b. Luminal phenotype of lineage-marked CARNs				
Marker	**Cell type**	**# CARNs examined**	**# Mice**	**# CARNs expressing**
p63	basal	98	3	0 *(0%)*
Cytokeratin 14	basal	131	4	0 *(0%)*
Cytokeratin 5	basal	93	4	2 *(2%)*
Cytokeratin 18	luminal	123	4	123 *(100%)*

3. CARNs are bipotential			
Progeny of lineage-marked CARNs in regenerated prostate	**# YFP$^+$ cells (lineage-marked progeny)**	**# Mice**	**# Basal YFP$^+$ cells (basal lineage-marked progeny)**
	559	4	17 *(3.0%)*

4. CARNs can self-renew			
Self-renewing lineage-marked CARNs in regressed prostate	**# Nkx3.1$^+$YFP$^+$ cells (lineage-marked CARNs)**	**# Mice**	**# Nkx3.1$^+$YFP$^+$BrdU$^+$ cells (self-renewing CARNs)**
	68	4	16 *(24%)*

5. CARNs can reconstitute prostate ducts after single-cell transplantation		
Grafted cells	**Grafts performed**	**Grafts recovered**
Single YFP-positive (lineage-marked CARN)	43	16 *(37%)* (p<0.001)
Single YFP-negative	31	1 *(3%)*

Supplementary Table 2. Analysis of self-renewal in CARNs.

Marker phenotype of cells in second round regressed state (Fig. 3a,b)		**Number of cells in category**				
		Animal analyzed				**Total** *(percent)*
Category of cells	**Interpretation**	**#1**	**#2**	**#3**	**#4**	
$Nkx3.1^+$	CARNs	100	64	337	417	**918** *(2.5%)*
YFP^+	Lineage-marked cells	169	108	330	378	**985** *(2.6%)*
$BrdU^+$	Proliferating cells	318	196	816	920	**2250** (*6.0%)*
$Nkx3.1^+YFP^+$	Lineage-marked CARNs (second round)	13	12	19	24	**68** *(0.18%)*
$Nkx3.1^+BrdU^+$	CARNs that have proliferated	14	24	58	70	**166** *(0.44%)*
YFP^+BrdU^+	Lineage-marked cells that have proliferated	27	20	35	45	**127** *(0.34%)*
$Nkx3.1^+YFP^+BrdU^+$	CARNs that have undergone a self-renewal division	3	2	5	6	**16** *(0.04%)*
Total epithelial cells		6259	3705	13484	14067	**37515**
Ratios of cell categories	**Interpretation**	**Percentages**				
$Nkx3.1^+BrdU^+/Nkx3.1^+$	Percentage of CARNs that have proliferated	14%	38%	17%	17%	**18%**
$Nkx3.1^+YFP^+BrdU^+/Nkx3.1^+YFP^+$	Percentage of lineage-marked CARNs that have undergone a self-renewal division	23%	17%	26%	25%	**24%**

Cells were counted in sections of anterior prostate from 4 different mice treated as shown in Fig. 3a,b. Regions enriched for CARNs ($Nkx3.1^+$ cells) were analyzed; thus the percentage of CARNs (2.5%) is higher than that determined by counting sections through the entire prostate.

Supplementary Table 3. Quantitation of BrdU label-retaining cells.

1. BrdU labeling efficiency immediately after labeling			
Mouse ID	**# BrdU$^+$ cells**	**# epithelial cells**	**% BrdU$^+$ cells/total epithelial cells**
0050	2,533	17,060	14.8%
0051	1,822	15,851	11.5%
0052	2,042	16,259	12.6%
0053	720	16,123	4.5%
Totals	7,117	65,293	10.9%
2. Percentage of LRCs after five rounds of serial regression			
Mouse ID	**# BrdU$^+$ cells**	**# epithelial cells**	**% BrdU$^+$ cells/total epithelial cells**
0501	92	6,588	1.4%
0502	151	15,388	1.0%
2006	224	11,110	2.0%
Totals	467	33,086	1.4%
3. Overlap of LRCs with CARNs			
Mouse ID	**# BrdU$^+$Nkx3.1$^+$ cells**	**# Nkx3.1$^+$ cells**	**% BrdU$^+$Nkx3.1$^+$/ Nkx3.1$^+$ cells**
0501	6	42	14.3%
0502	6	60	10.0%
2006	15	91	16.5%
Totals	27	193	14.0%
4. Percentage of LRCs after five rounds of serial regeneration			
a. Wild-type			
Mouse ID	**# BrdU$^+$ cells**	**# epithelial cells**	**% BrdU$^+$ cells/total epithelial cells**
1011	239	28,971	0.82%
4212	219	27,034	0.81%
4782	156	19,753	0.79%
Totals	614	75,758	0.81%
b. Nkx3.1$^{-/-}$ mutant			
Mouse ID	**# BrdU$^+$ cells**	**# epithelial cells**	**% BrdU$^+$ cells/total epithelial cells**
0909	36	24,602	0.15%
0911	35	14,048	0.25%
8371	89	15,394	0.58%
8372	66	15,903	0.48%
8373	46	16,654	0.28%
Totals	272	86,601	0.31% (p=0.003)

Supplementary Table 4. Summary of prostate phenotypes in control and *Nkx3.1* mutant mice after three and five rounds of serial regression/regeneration.

***Nkx3.1* genotype**	**Regeneration**	**Number**	**Normal**	**Hyperplasia**	**PIN**
+/+	3 rounds	7	4	2	1
+/+	5 rounds	9	8	1	0
+/+	Intact[a]	6	4	1	1
+/–	3 rounds	8	3	5	0
+/–	5 rounds	8	7	1	0
+/–	Intact[a]	7	2	2	3
–/–	3 rounds	5	0	5	0
–/–	5 rounds	10	3	7	0[b]
–/–	Intact[a]	9	3	1	5

Phenotypes were scored blind using hematoxylin-eosin stained anterior prostate sections, using standard criteria[1].

[a]Data for intact mice at 6-12 months of age have been previously published[2].

[b]Difference in frequency of PIN between serially regenerated and intact *Nkx3.1* homozygous animals is significant ($p < 0.01$).

Supplementary Table 5. Antibodies used in this study.

Antigen	Supplier	Ig type	Dilution
Androgen receptor	Sigma #A9853	rabbit IgG	1:500
Androgen receptor (AN1-15)	Affinity Bioreagents MA1-150	rat IgG	1:50
β-catenin	BD Biosciences #610153	mouse IgG1	1:1000
β-galactosidase	Rockland #100-4136	rabbit IgG	1:1000
BrdU	Abcam #ab1893	sheep IgG	1:200
CK5	Covance #PRB-160P	rabbit IgG	1:500
CK14	Biogenex #MU146-UC	mouse IgG1	1:100
CK18	Abcam #ab668	mouse IgG1	1:100
CD117 (ACK2)	eBioscience #14-1172	rat IgG2b	1:100
CD117 (ACK45)	BD Pharmingen #553868	rat IgG2b	1:100
Cre	Covance #PRB-106C	rabbit IgG	1:1000
E-cadherin	Cell Signaling #4046	rabbit IgG	1:200
GFP	Invitrogen #A11122	rabbit IgG	1:1000
GFP	Roche #11814460001	mouse IgG1	1:200
GFP	Abcam #ab13970	chick IgY	1:1000
Ki67	DakoCytomation #M7249	rat IgG2a	1:600
Ki67	Novocastra #NCL-Ki67p	rabbit IgG	1:1400
Nkx3.1	Ref. 3	rabbit IgG	1:1000 or 1:8000
Nkx3.1	Ref. 4	rabbit IgG	1:2000
p63	Santa Cruz #sc-8431	mouse IgG1	1:600
p63	Santa Cruz #sc-8343	rabbit IgG	1:50
PTEN	Cell Signaling #9559	rabbit IgG	1:100
Phospho-Akt	Cell Signaling #3787	rabbit IgG	1:50
Smooth muscle actin	Sigma #A2547	mouse IgG1	1:300
Synaptophysin	Zymed #18-0130	rabbit IgG	1:500

References for supplementary material

[1] Park, J.H. *et al.*, Prostatic intraepithelial neoplasia in genetically engineered mice. *Am J Pathol* 161 (2), 727-735 (2002).

[2] Kim, M.J. *et al.*, Nkx3.1 mutant mice recapitulate early stages of prostate carcinogenesis. *Cancer Res.* 62 (11), 2999-3004 (2002).

[3] Kim, M.J. *et al.*, Cooperativity of Nkx3.1 and Pten loss of function in a mouse model of prostate carcinogenesis. *Proc. Natl. Acad. Sci. USA* 99 (5), 2884-2889 (2002).

[4] Chen, H., Mutton, L.N., Prins, G.S., & Bieberich, C.J., Distinct regulatory elements mediate the dynamic expression pattern of Nkx3.1. *Dev Dyn* 234 (4), 961-973 (2005).

[5] Bunting, M., Bernstein, K.E., Greer, J.M., Capecchi, M.R., & Thomas, K.R., Targeting genes for self-excision in the germ line. *Genes Dev.* 13 (12), 1524-1528 (1999).

[6] Cunha, G.R. & Vanderslice, K.D., Identification in histological sections of species origin of cells from mouse, rat and human. *Stain Technol* 59 (1), 7-12 (1984).

[7] Lei, Q. *et al.*, NKX3.1 stabilizes p53, inhibits AKT activation, and blocks prostate cancer initiation caused by PTEN loss. *Cancer Cell* 9 (5), 367-378 (2006).

Legends for Supplementary Figures

Supplementary Figure 1. Expression of Nkx3.1 and CD117 (c-kit) in prostatic lobes of androgen-deprived mice. a, Confocal immunofluorescence detection of Nkx3.1 and p63 in wild-type intact anterior prostate; nuclei are detected by counter-staining with TOPRO3. Representative Nkx3.1^{+} luminal (lum) and p63^{+} basal (bas) cells are indicated; arrow indicates a basal cell that co-expresses Nkx3.1 and p63. **b,** Expression of Nkx3.1 and p63 in wild-type anterior prostate after one round of regression and regeneration. Arrow indicates a basal cell that co-expresses Nkx3.1 and p63. **c, d,** Detection of castration-resistant Nkx3.1-expressing cells (CARNs) (arrows) in ventral prostate (VP) (**c**) and dorsolateral prostate (DLP) (**d**) of a castrated adult male. **e, f,** Detection of CARNs (arrows) in anterior prostate (AP) (**e**) and dorsolateral prostate (**f**) in the second-round regressed state, following one round of regeneration and regression. **g,** Expression of androgen receptor (AR) by a CARN (arrow) in the regressed prostate. **h,** CARNs are growth-quiescent, as shown by lack of co-staining for Nkx3.1 (arrows) and Ki67 (arrowheads) in regressed prostate. **i,** Detection of CARNs (arrows) in wild-type prostate using an independent Nkx3.1 polyclonal antiserum[4]. **j,** Absence of Nkx3.1 immunostaining in a *Nkx3.1*$^{-/-}$ homozygous mutant anterior prostate. **k, l,** Expression of CD117 (c-kit) in the regressed anterior prostate, as detected by two different monoclonal antibodies, ACK2 (**k**) and ACK45 (**l**). Note that the rare CD117-positive cells are never luminal. Scale bars correspond to 25 microns.

Supplementary Figure 2. Generation and analysis of the inducible *Nkx3.1*$^{CreERT2/+}$ knock-in allele in intact male mice. a, The targeting strategy utilizes the self-excising *ACE-Cre/PolII-neo* selection cassette from the pACN vector[5], and inserts *CreER*^{T2}*-polyA* at the translation start site for *Nkx3.1,* thereby generating a null allele for *Nkx3.1.* Excision of the selection cassette by *Cre-loxP* recombination occurs by passage through the male germline, and occurs with 100% efficiency. *Abbreviations:* E, *Eco*RI; H, *Hin*DIII; X, *Xba*I. **b,** The CreER^{T2} fusion protein is inactive unless transiently activated by tamoxifen. Cre activation can lead to recombination at the

R26R-lacZ reporter locus; since this occurs on a cell-by-cell basis, the resulting tissue may be mosaic for *lacZ* expression. **c, d,** Low-power views of β-galactosidase staining of dorsolateral prostate from intact *Nkx3.1*$^{CreERT2/+}$*; R26R-lacZ/+* mice, either mock-injected (**c**) or injected with tamoxifen (**d**). **e, f,** Cre-mediated recombination in the anterior prostate of intact *Nkx3.1*$^{CreERT2/+}$*; R26R-YFP/+* mice following tamoxifen-induction, showing sporadic YFP expression predominantly in luminal cells (**e**), but also in p63^{+} basal cells (arrow, **f**). Scale bars correspond to 100 microns (**c, d**) or 25 microns (**e, f**).

Supplementary Figure 3. Bipotentiality and self-renewal of CARNs. a, Co-localization of YFP (arrows) and cytokeratin 14 is not observed in the castrated and tamoxifen-induced *Nkx3.1*$^{CreERT2/+}$*; R26R-YFP/+* anterior prostate (n=0/131 YFP^{+} cells). **b,** Co-localization of YFP with cytokeratin 5 (CK5) is almost never observed (n=2/93 YFP^{+} cells); both of the observed YFP^{+}CK5^{+} cells show atypical basal morphology (*inset*). **c,** Co-localization of YFP with cytokeratin 18 (CK18) (n=123/123 YFP^{+} cells). **d,** Co-expression of YFP with androgen receptor (AR) (n=94/94). **e,** Overlap of Cre and YFP expression (arrows) in castrated and tamoxifen-induced *Nkx3.1*$^{CreERT2/+}$*; R26R-YFP/+* anterior prostate at four days following tamoxifen administration in the regressed state. **f,** Persistence of lineage-marked cells (arrows) in the androgen-deprived and tamoxifen-induced *Nkx3.1*$^{CreERT2/+}$*; R26R-YFP/+* prostate epithelium, using direct visualization of YFP. Mice were castrated at two months of age and tamoxifen-induced after four weeks of regression, then maintained in the androgen-deprived state until analysis at ten months of age. **g-i,** Co-localization of YFP and p63 in a lineage-marked basal cells (arrow) of a castrated, tamoxifen-induced, and regenerated *Nkx3.1*$^{CreERT2/+}$*; R26R-YFP/+* anterior prostate, shown as an overlay (**g**) and as individual channels (**h, i**).**j-l,** Co-localization of β-galactosidase and cytokeratin 14 in a lineage-marked basal cell (arrow) of a castrated, tamoxifen-induced, and regenerated *Nkx3.1*$^{CreERT2/+}$*; R26R-lacZ/+* anterior prostate, shown as an overlay (**j**) and as individual channels (**k, l**). **m,** Strategy for analysis of self-renewal. *Nkx3.1*$^{CreERT2/+}$*; R26R-*

YFP/+ male mice are castrated, tamoxifen-induced, and regenerated, with BrdU administered during the first three days of regeneration, followed by removal of androgens and prostate regression. Triple-positive $Nkx3.1^{+}YFP^{+}BrdU^{+}$ cells would correspond to cells that were CARNs in both the first and second regressions, and had undergone proliferation, consistent with self-renewal. Scale bars correspond to 25 microns.

Supplementary Figure 4. Generation of prostate tissue by dissociated CARNs in tissue recombinants. a, Strategy for analysis of CARNs potential in tissue recombinant/renal grafts generated using approximately 160 lineage-marked YFP^{+} cells. **b-d,** Contribution of lineage-marked YFP^{+} cells in renal grafts grown from dissociated cells of castrated and tamoxifen-induced *Nkx3.1*$^{CreERT2/+}$*; R26R-YFP/+* mice combined with rat urogenital mesenchyme. The percentage of lineage-marked basal cells varies significantly in these grafts; compare their relative absence in **b** (arrowheads indicate non-marked basal cells) to their abundance in **d**. **e-g,** Higher-power view of duct in **d** shows numerous $YFP^{+}p63^{+}$ basal cells (arrows); *insets* show co-localization of YFP and p63. Scale bars correspond to 25 microns.

Supplementary Figure 5. Generation of prostatic ducts in renal grafts by single lineage-marked CARNs. a-f, Bright-field (**a, b**) and epifluorescence (**d, e**) views of dissociated prostate cells from lineage-marked *Nkx3.1*$^{CreERT2/+}$*; R26R-YFP/+* prostate tissue (**a, d**) and single YFP^{+} cells isolated by mouth-pipetting (**b, e**). Dark-field (**c**) and epifluorescence (**f**) views of renal grafts after growth for 2.5 months. **g, h,** Expression of E-cadherin (**g**) and cytokeratin 5 (CK5) (**h**) in ducts from single YFP^{+} cells. Scale bars correspond to 25 microns (**a, b, d, e, g, h)** or 1 mm (**c, f**).

Supplementary Figure 6. Distinct morphology of mouse and rat nuclei in renal grafts. High-power images of DAPI-stained ducts from tissue recombinants/renal grafts show that mouse nuclei (**a**) contain multiple punctate staining regions, while rat nuclei (**b**) generally do not[6]. Note that the epithelium from the single-cell graft in **a** contains mouse epithelium (epi) and rat stroma (str) as expected, while both the epithelium and stroma in **b** are of rat origin.

Supplementary Figure 7. Histopathological analysis of wild-type and *Nkx3.1*$^{-/-}$ mutant prostates after three rounds of serial regression/regeneration. a, Timeline for serial regression/regeneration strategy. **b-e,** Immunostaining for the basal cell marker p63 in wild-type (**b, d**; arrow, **d**) and *Nkx3.1*$^{-/-}$serially-regenerated mutant prostate (**c, e**; arrow, **e**); note that an area of the *Nkx3.1*$^{-/-}$ prostate in (**c**) lacks epithelial cells (arrows). **f, g,** α-smooth muscle actin (SMA) marks stroma in wild-type (**f**) and *Nkx3.1*$^{-/-}$ (**g**) serially-regenerated prostate; no difference in staining pattern is observed. **h, i,** Nkx3.1 immunostaining is detected in wild-type (**h**), but not *Nkx3.1*$^{-/-}$ (**i**) mutant prostate after three rounds of serial regeneration. Scale bars correspond to 50 microns.

Supplementary Figure 8. Histopathological analysis of wild-type and *Nkx3.1*$^{-/-}$ mutant prostates after five rounds of serial regression/regeneration. a, Timeline for serial regression/regeneration strategy. **b-e,** Hematoxylin-eosin staining of wild-type (**b, d**) and *Nkx3.1*$^{-/-}$ mutant (**c, e**) anterior prostate after serial regeneration, shown at low (**b, c**) and high-power (**d, e**). Note the relative absence of epithelial hyperplasia typically found in intact *Nkx3.1*$^{-/-}$ mutants, as well as an increase in basal cells in limited regions (arrow, **e**). **f, g,** Increased number of p63^{+} basal cells (arrow, **g**) in regions of serially regenerated *Nkx3.1*$^{-/-}$ mutant prostates. **h, i,** Similar proliferative index in serially regenerated wild-type (**h**) and *Nkx3.1*$^{-/-}$ mutant (**i**) anterior prostates, as determined by Ki67 immunostaining (arrows). **j, k,** α-smooth muscle actin (SMA) marks stroma in wild-type and *Nkx3.1*$^{-/-}$ serially-regenerated anterior prostate. No difference in staining

patterns is observed, in contrast with the significantly attenuated SMA staining in intact *Nkx3.1*$^{-/-}$ mutant prostate at similar ages[2]. **l, m,** Androgen receptor (AR) immunostaining shows an identical pattern in wild-type (**l**) and *Nkx3.1*$^{-/-}$ (**m**) serially-regenerated anterior prostate. Note that AR immunoreactivity is modestly increased in *Nkx3.1*$^{-/-}$ mutant prostate epithelium, as has been previously reported for intact mice[7]. **n, o,** Nkx3.1 immunostaining can be detected in wild-type (**n**), but not *Nkx3.1*$^{-/-}$ (**o**) mutant prostate after five rounds of serial regeneration. **p, q,** Synaptophysin (Syn) immunoreactivity detects rare neuroendocrine cells in serially regenerated wild-type (**p**) and *Nkx3.1*$^{-/-}$ mutant (**q**) anterior prostates. **r, s,** Hematoxylin-eosin (H&E) staining of dorsolateral (DLP) prostate shows that the phenotype of the serially regenerated *Nkx3.1*$^{-/-}$ mutant DLP (**r**) resembles that of the wild-type DLP control (**s**). Scale bars correspond to 100 microns (**b-g**) or 50 microns (**h-s**).

Supplementary Figure 9. Model for *Nkx3.1* function in prostate stem cell maintenance. Note that for simplicity, stem cells and multipotent progenitors (MPP) are not depicted as either luminal or basal. **a,** In intact *Nkx3.1* mutant mice, stem cell self-renewal may be impaired, leading to increased differentiation of lineage-restricted transit amplifying cells and consequent epithelial hyperplasia. **b,** Depletion of stem cells and transit amplifying cells through serial regression/regeneration would lead to reversion of the hyperplasia phenotype due to androgen-dependent apoptosis of luminal cells during regression, accompanied by potential accumulation of androgen-independent basal cells.

Supplementary Figure 1.

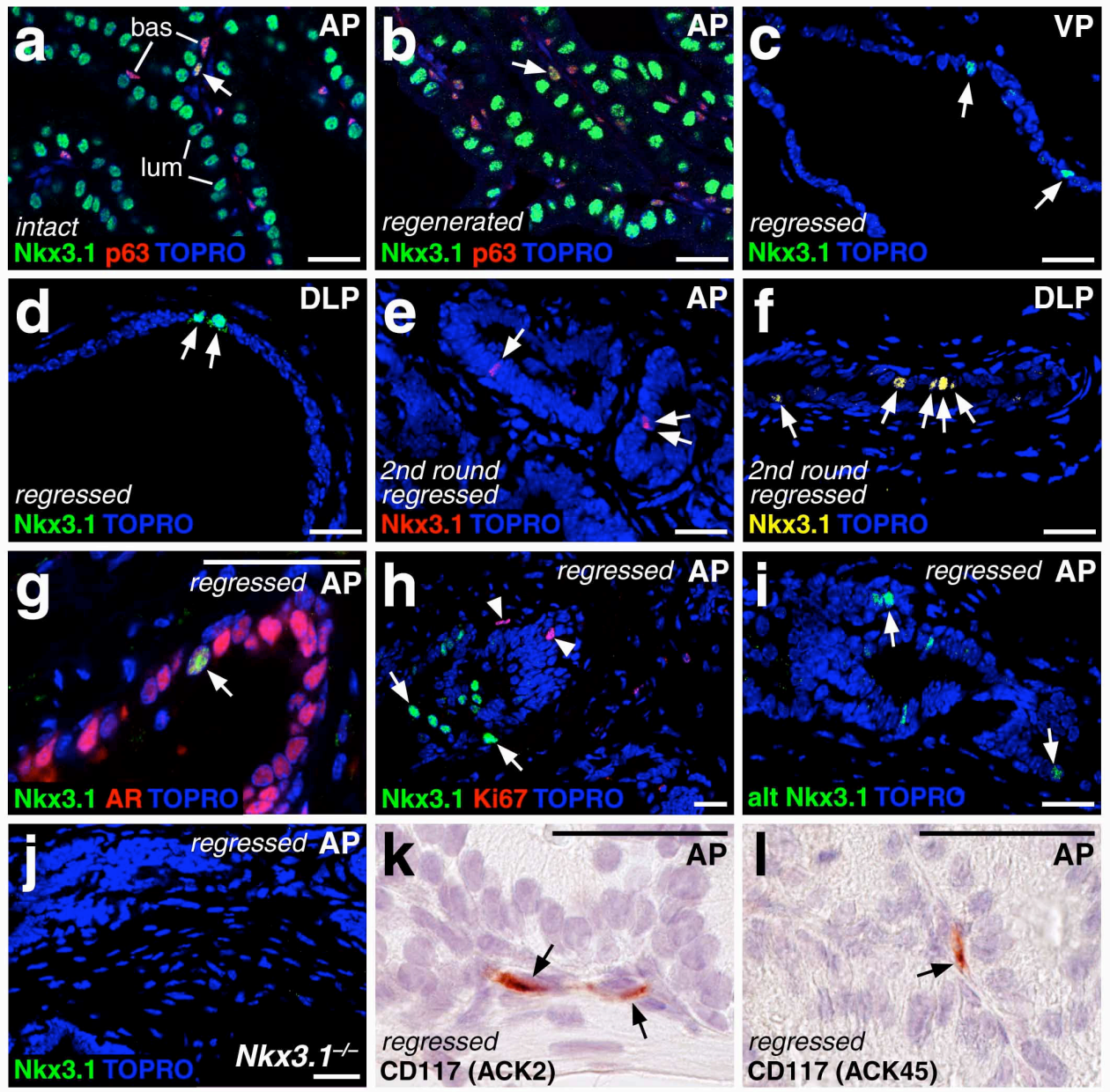

Supplementary Figure 2.

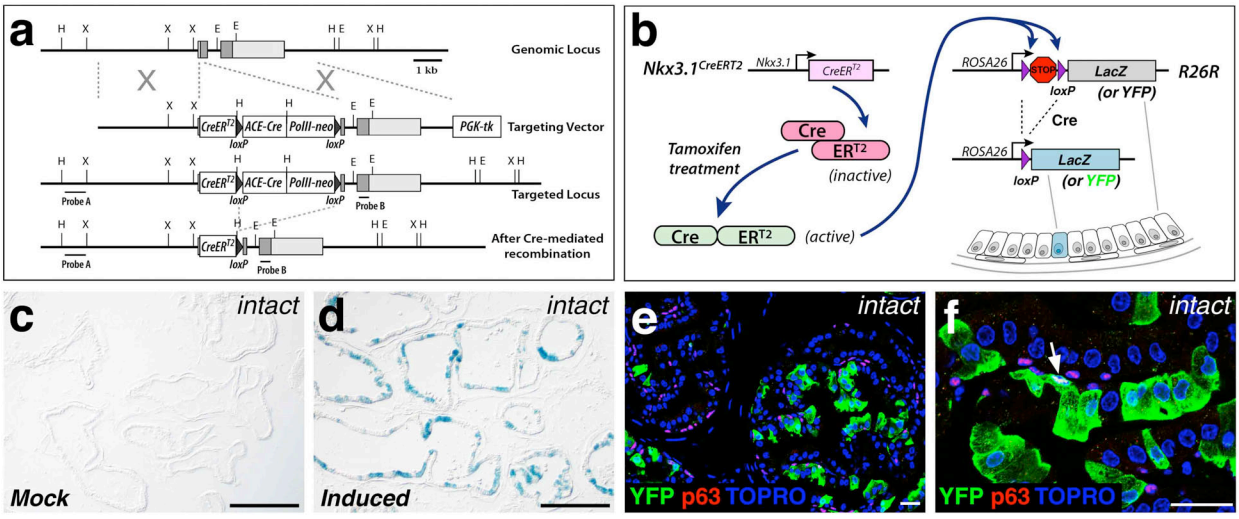

Supplementary Figure 3.

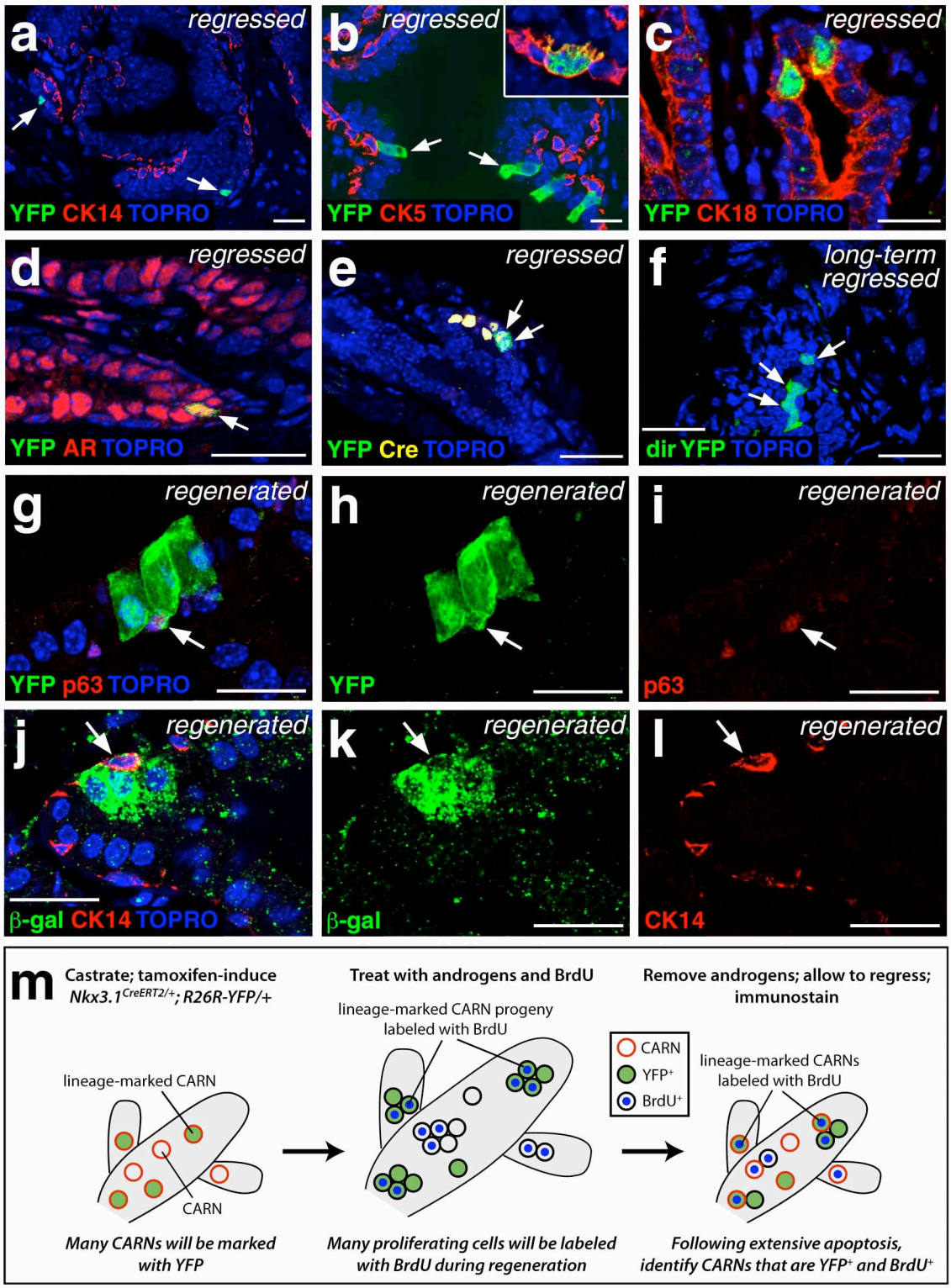

Supplementary Figure 4.

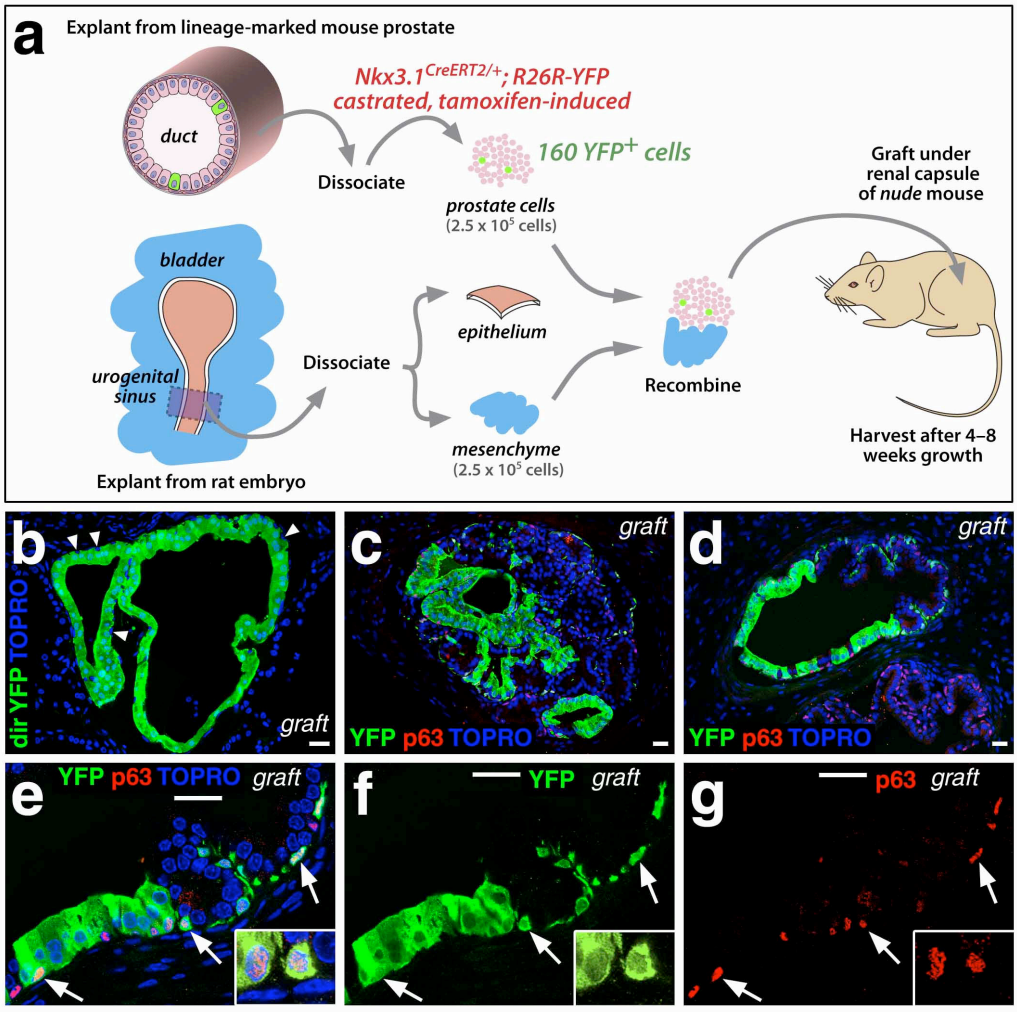

Supplementary Figure 5.

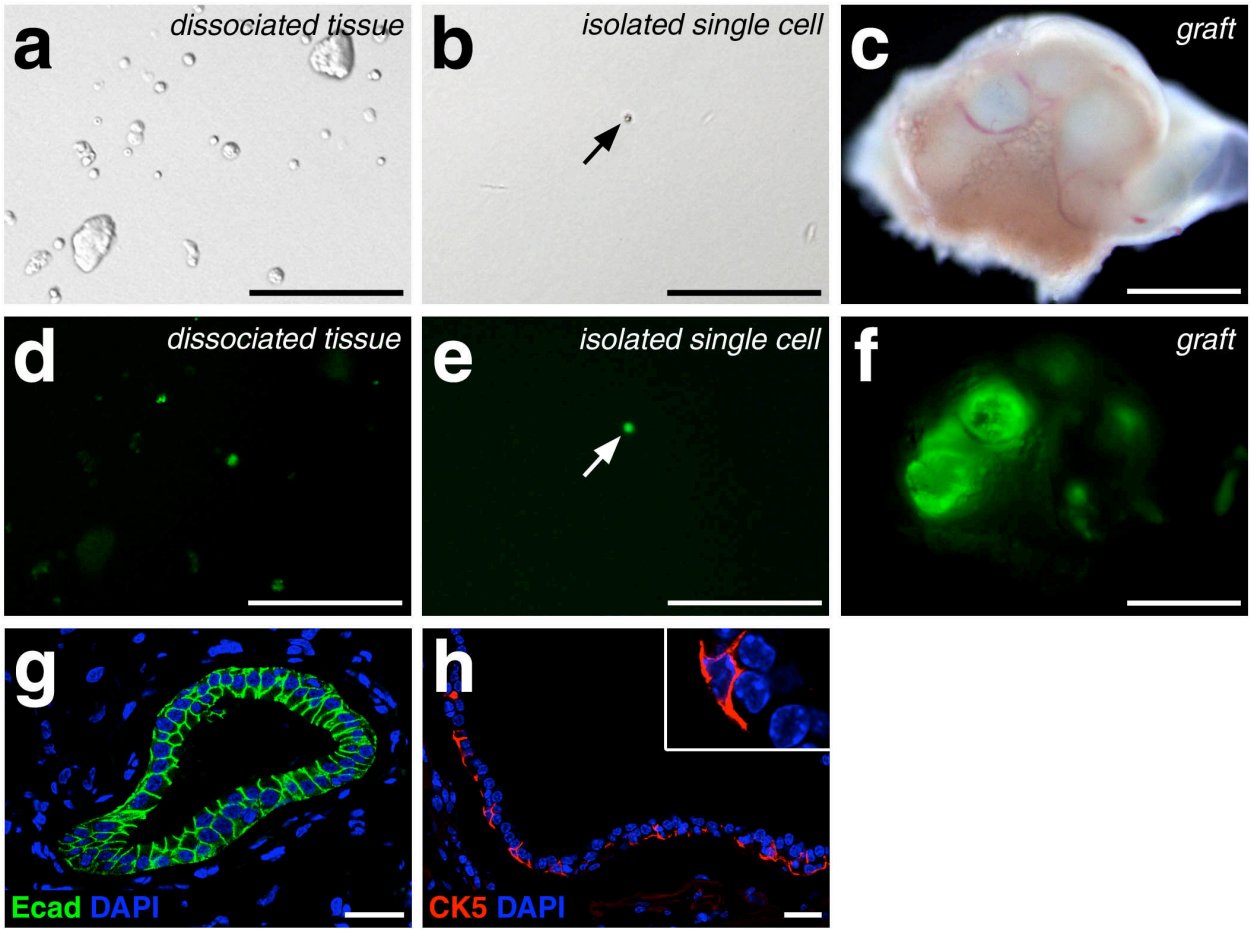

Supplementary Figure 6.

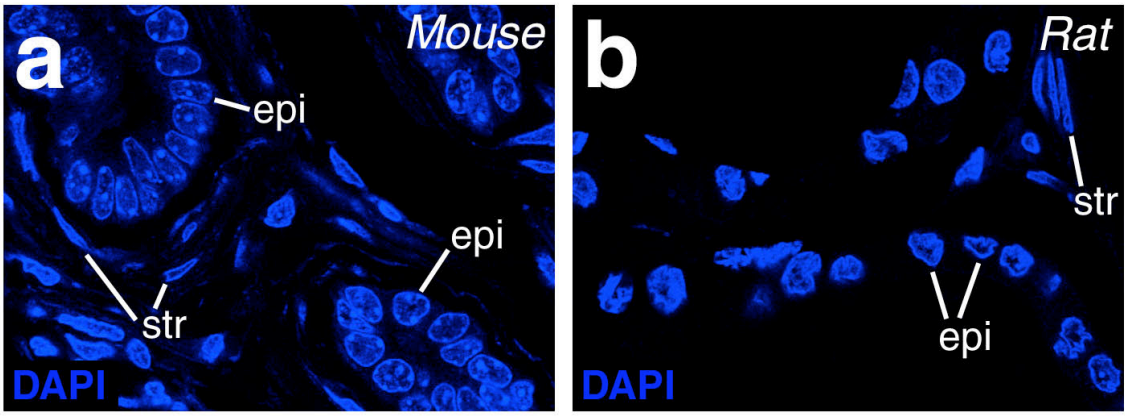

Supplementary Figure 7.

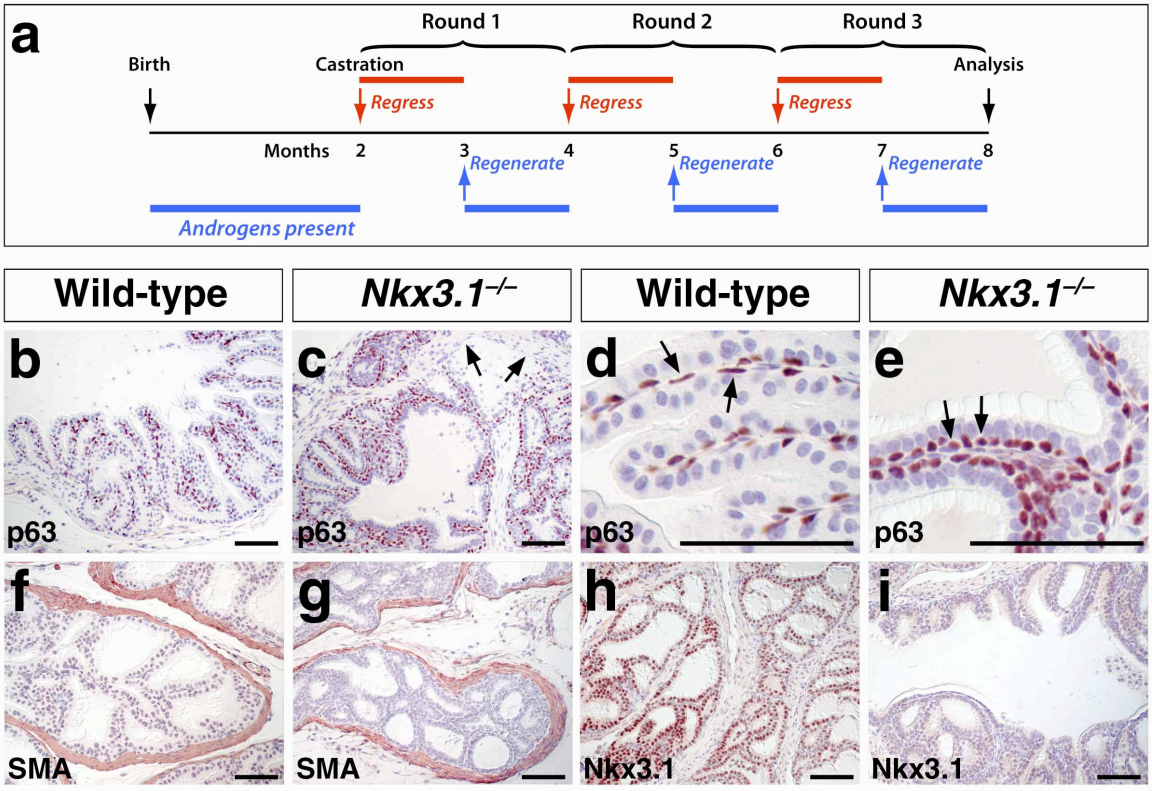

Supplementary Figure 8.

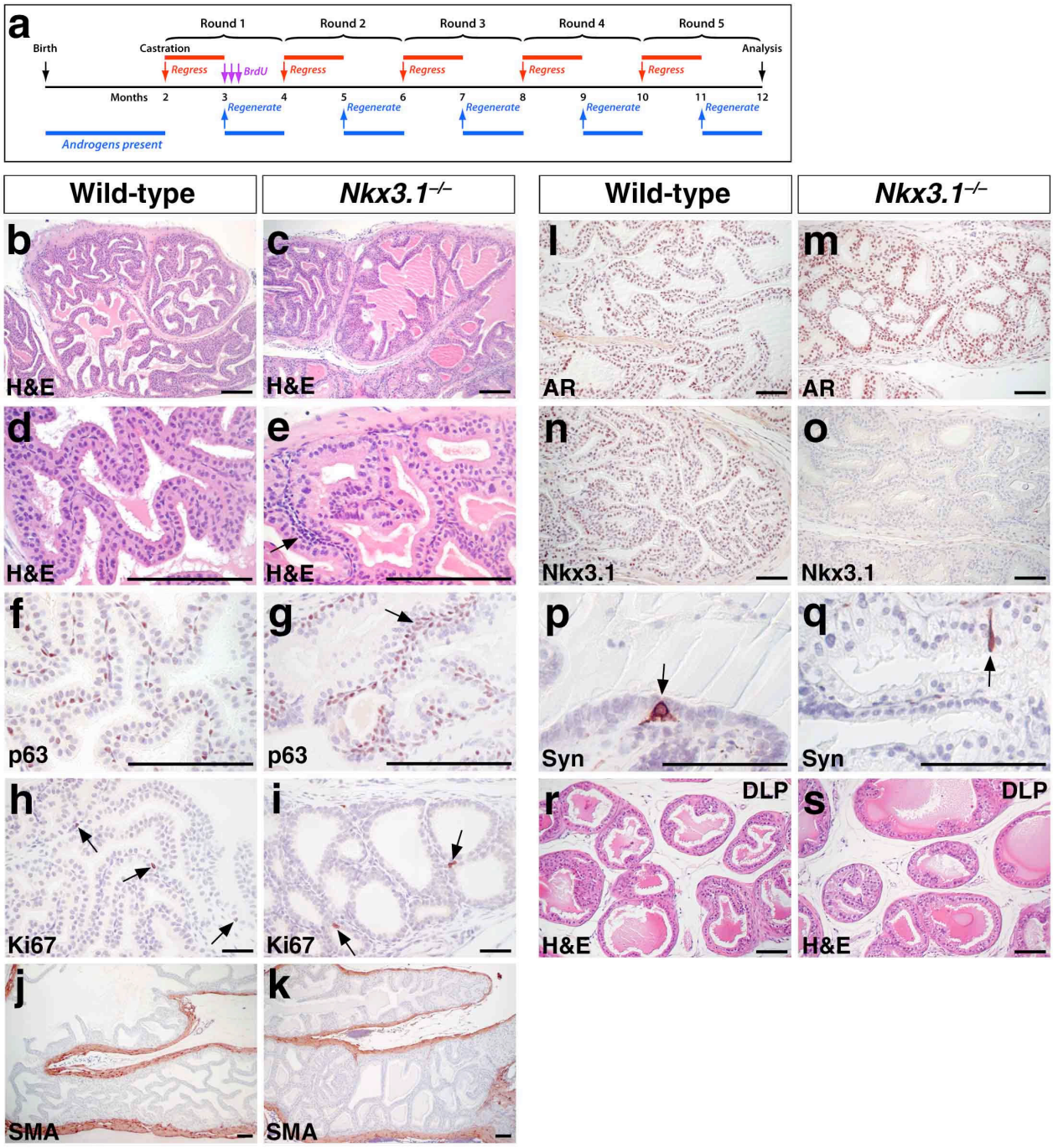

Supplementary Figure 9.